HHS Public Access

Author manuscript

J Immunol. Author manuscript; available in PMC 2018 October 01.

Published in final edited form as:

J Immunol. 2017 October 01; 199(7): 2305–2315. doi:10.4049/jimmunol.1700833.

ADAM10-mediated ICOSL Shedding on B cells is Necessary for Proper T cell ICOS Regulation and T_{FH} Responses

Joseph C Lownik[1,¥], **Andrea J. Luker**[2,¥], **Sheela R. Damle**[2], **Lauren Folgosa Cooley**[1], **Riham El Sayed**[3,4], **Andreas Hutloff**[4], **Costantino Pitzalis**[3], **Rebecca K. Martin**[2,*], **Mohey Eldin M El Shikh**[3,*], and **Daniel H. Conrad**[2,*]

[1]Center for Clinical and Translational Research, School of Medicine, Virginia Commonwealth University, Richmond, Virginia 23298, USA

[2]Department of Microbiology and Immunology, School of Medicine, Virginia Commonwealth University, Richmond, Virginia 23298, USA

[3]Experimental Medicine and Rheumatology, William Harvey Research Institute, Queen Mary University of London, Charterhouse Square campus, London EC1M 6BQ, United Kingdom

[4]Department of Clinical and Chemical Pathology, Kasr Al-Ainy Faculty of Medicine, Cairo University, Egypt

[5]German Rheumatism Research Centre Berlin, 10117 Berlin, Germany

Abstract

The proper regulation of inducible costimulator (ICOS) and its ligand (ICOSL) have been shown to be essential for maintaining proper immune homeostasis. Loss of either protein results in defective humoral immunity, and overexpression of ICOS results in aberrant antibody production resembling lupus. How ICOSL is regulated in response to ICOS interaction is still unclear. We demonstrate that ADAM10 is the primary physiological sheddase of ICOSL in both mouse and human. Using an *in vivo* system in which ADAM10 is deleted only on B cells ($ADAM10^{B-/-}$), elevated levels of ICOSL were seen. This increase is also seen when ADAM10 is deleted from human B cell lines. Identification of the primary sheddase has allowed the characterization of a novel mechanism of ICOS regulation. In wildtype (WT) mice, interaction of ICOSL/ICOS results in ADAM10 induced shedding of ICOSL on B cells and moderate ICOS internalization on T cells. When this shedding is blocked, excessive ICOS internalization occurs. This results in severe defects in T follicular helper (T_{FH}) development and T_H2 polarization, seen in a house dust mite exposure model. In addition, enhanced T_H1 and T_H17 immune responses are seen in experimental allergic encephalomyelitis. Blockade of ICOSL rescues T cell ICOS surface expression and at least partially rescues both T_{FH} numbers and the abnormal antibody production previously reported in these mice. Overall, we propose a novel regulation of the ICOS/ICOSL axis, with ADAM10 playing a direct role in regulating ICOSL as well as indirectly regulating ICOS, thus controlling ICOS/ICOSL-dependent responses.

¥These authors have contributed equally to this work and are designated as first authors.

*Co-senior authors.

Introduction

A Disintegrin And Metalloproteinases (ADAMs) are a family of zinc-dependent proteinases which can mediate intramembrane proteolysis and ectodomain shedding of membrane proteins. Of the ADAM family proteins, the proteolytic domains of ADAM10 and ADAM17 share the highest homology, often resulting in the ability to cleave overlapping substrates (1, 2). ADAM10 has been shown to act in many paracrine signaling mechanisms and is responsible for cleaving numerous substrates, including Notch receptors, Delta-like 1 (Dll1), IL-6R, CXCL16, and CD23 (3, 4). We have shown that loss of ADAM10 on B cells ($ADAM10^{B-/-}$) results in loss of the marginal zone B cell compartment, disorganized secondary lymphoid architecture, decreased antigen-specific antibody (5), and decreased airway hyper-responsiveness and eosinophilic infiltration in two models of allergic airway disease (6, 7).

Inducible costimulatory (ICOS) on T cells and its ligand (ICOSL) which is expressed on antigen-presenting cells (APCs) have been shown to be essential for T follicular helper (T_{FH}) and T_H2 development and activity (8–11). T_{FH} cells are essential for productive germinal center (GC) responses, providing help to B cells undergoing class switch recombination and somatic hypermutation as well as being critically involved in GC B cell differentiation into memory B cells and long lived plasma cells (8, 12). Deficiency of either ICOS or ICOSL essentially abolishes T-dependent humoral immune responses (9, 11). There have been several studies illustrating the regulation of ICOS (13–15), particularly at the mRNA level, as well as the cleavage of ICOSL. In particular, ADAM17, was shown to cleave ICOSL in response to Phorbol Myristate Acetate (PMA) and B cell receptor (BCR) crosslinking (16). However, ADAM17 was not involved in ICOS-induced shedding of ICOSL and constitutive ICOSL levels were unchanged. This indicates a second, unknown protease is involved in physiological B cell activation in the germinal centers as well as the cross talks between ICOS and ICOSL. Given these data, understanding the regulation of these proteins is quite important.

Here we identify the physiologically relevant ICOSL sheddase to be ADAM10. We show that while both recombinant ADAM10 and ADAM17 can cleave recombinant ICOSL, only $ADAM10^{B-/-}$ mice have significantly elevated ICOSL on B cells. Loss of both proteases in B cells ($ADAM10/17^{B-/-}$) marginally increases ICOSL levels over the loss of ADAM10 alone, suggesting a secondary role in ICOSL regulation for ADAM17. In these mice, the overexpression of surface ICOSL results in the internalization and degradation of T cell ICOS in the absence of T cell receptor (TCR) stimulation. As a result, the mice lack both proper T_{FH} and T_H2 effector cell populations post immunization, explaining the defective humoral immunity previously reported in the $ADAM10^{B-/-}$ mice (5, 6). In addition, increased ICOSL resulted in enhanced T_H1 and T_H17 T cell activation as demonstrated by a model of Experimental Autoimmune Encephalitis (EAE). Overall, these studies not only identify the sheddase of ICOSL following ICOS interaction, but also present a novel mechanism of ICOS regulation at the post-translational level. We hypothesize that ligand:receptor interaction causes ICOS internalization following ICOSL shedding by ADAM10. Interfering with this normal regulation gives rise to a phenotype similar to that seen in $ICOS^{-/-}$ mice.

Materials and Methods

Mice

Mice were maintained at the Virginia Commonwealth University Animal Facility in accordance with guidelines by the U.S. National Institutes of Health and American Association for the Accreditation of Laboratory Animals Care. C57BL/6 ADAM10$^{B-/-}$ mice were generated as previously described (3). In short, loxP sites were inserted to flank exon 9 of *Adam10*, and these mice were crossed to *Cd19*-Cre mice (Jackson 006785). *Adam17* floxed mice were purchased from Jackson (009597) and crossed to *Cd19*-Cre mice (006785). ADAM17$^{B-/-}$ mice were purchased from Jackson. ADAM10/17$^{B-/-}$ were generated by crossing ADAM10$^{B-/-}$ and ADAM17$^{B-/-}$ mice. Cre-recombinase negative littermates were used as wildtype controls.

RNA isolation and qPCR

For RNA isolation from cells, cell suspensions were centrifuged at 500 x g for 5 minutes, washed once with PBS and centrifuged again. TRIzol (Invitrogen) was used for RNA extraction per manufacturer's instructions. For RNA isolation from tissues, tissues were flash frozen in liquid nitrogen. TRIzol was added to frozen tissue and homogenized. Subsequent RNA isolation was performed to the manufacturer's instructions. RNA was quantified using an ND-100 Nanodrop spectrophotometer. 1μg of total RNA was reverse transcribed using SuperScript IV (ThermoFisher) with oligo(dT_{20}). Primers used in qPCR analysis are as follows: *Hprt*_foward 5′-CAGGGATTTGAATCACGTTTGTG-3′, *Hprt*_reverse 5′-TTGCAGATTCAACTTGCGCT-3′, *Icosl*_forward 5′-CAGCGGCATTCGTTTCCTTC-3′, *Icosl*_reverse 5′-GTCAGGCGTGGTCTGTAAGT-3′, *Icos*_forward 5′-TCTAGACTTGCAGGTGTGACC-3′, *Icos*_reverse 5′-CAGGGGAACTAGTCCATGCG-3′. In short, qPCR was conducted using a Quant Studio 3 (Applied Biosystems) with 45 cycles using PowerUp Sybr Green (Applied Biosystems). Primers were tested for specificity using melt curve analysis.

Flow Cytometry and ImageStream Analysis

Single cell suspensions were created and passed through a 40um strainer. For flow cytometry of spleens, red blood cells were lysed using ACK lysis buffer (Quality Biologic). 2μg anti-mouse CD16/32 (Biolegend; clone 93) was used to block Fc receptors. Fluorophore or biotinylated antibodies were used at manufacturers' recommended quantity; PE anti-IL4 (clone 11B11, Biolegend), PE/Cy7 anti-IL13 (clone eBio13A, eBioscience), APC and PE/Cy7 anti-CD45R/B220 (Clone RA3-6B2, Biolegend), APC and FITC anti-CD4 (clone GK1.5, Biolegend), PE anti-ICOS (clone C398.4A, Biolegend), PE anti-ICOSL (clone HK5.3, Biolegend), Biotin anti-CXCR5 (clone L138D7, Biolegend), Streptavidin PE/Cy7 (Biolegend), BV421 anti-PD1 (clone 29F.1A12, Biolegend), PE anti-human ICOSL (clone 2D3, Biolegend), PE anti-CD40 (HM40-3, Biolegend), APC anti-OX40L (clone HM40-3, Biolegend), PE/Cy7 anti-CD86 (clone GL-1, Biolegend), PE/Cy5 anti-CD80 (clone 16-10A1, Biolegend), PE/Cy7 anti-CD8a (clone 53-6.7, Biolegend), PE anti-CD3e (clone 145-2C11, Biolegend), FITC anti-CD44 (clone IM7, Biolegend), APC anti-CD45.1 (clone A20, Biolegend), AlexaFluor 647 anti-GL7 (clone GL7, Biolegend), PE anti-CD95 (clone 15A7, eBioscience), AlexaFluor 647 anti-IFNγ (clone XMG1.2, Biolegend), BV650 anti-

IL17A (clone TC11-18H10, BD). Flow cytometry data was analyzed using FSC Express 5. For intracellular cytokine staining from lung and draining lymph nodes, cells were stimulated using an anti-CD3 coated plate (1μg/mL) for 4 hours in the presence of monensin. Cells were fixed and permeabilized and stain for indicated targets. Data was acquired using LSR Fortessa for flow cytometry and Amnis ImageStream. Internalization index was calculated using IDEAS 6.0 software.

Shedding Assays

B cells isolated from spleens of indicated strains were stimulated with the following: 25ng/mL PMA, 2μM ionomycin, 50μg/mL HLA, 2.5μg/mL plate-bound ICOS or vehicle controls for each. Cells were stimulated for 1 hour at 37°C in complete RPMI. Following stimulation, cells were washed 2 times with cold PBS. Cells were stained for surface ICOSL for 30 minutes on ice following Fc-receptor blocking. Cells were washed twice with staining buffer and fixed using 2% PFA and analyzed by flow cytometry. %ICOSL shed as calculated as [(Unstimulated ICOSL MFI – Stimulated ICOSL MFI) / (Unstimulated ICOSL MFI).

Recombinant Cleavage Assays

Recombinant His-tagged mouse ICOS-L (100ng; R&D #8127-B7) and rmADAM10 (1 μg, R&D 946-AD) or ADAM17 (1μg, R&D 2978-AD) were incubated together for 24 hours at 37 degrees. To remove N-linked glycosylation, cleaved samples were treated with PNGase F under denaturing conditions according to manufacturer's instructions (New England Biolabs). SDS Samples were reduced and run on 12% Bis-Tris gels before transfer onto nitrocellulose blots. Anti-ICOSL (Sino Biologic, 50190-RP01) and anti-His Tag (Biolegend, clone J099B12) were diluted 1:1000 and incubated for 1 hour at room temperature. Secondary antibodies (Goat anti-mouse IgG1, Goat anti-Rabbit IgG, both Southern Biotech) were conjugated to HRP and diluted 1:10,000 in 5% milk block and incubated for 1 hour at room temperature. Blots were developed using ECL Western Blotting Substrate (Pierce) and read using a Biorad GelDoc system.

NP-KLH Immunizations

For footpad immunizations, 10μg of 4-hydroxy-3-nitrophenylacetatyl hapten conjugated to keyhole limpet hemocyanin (NP_{31}-KLH; BioSearch Technologies) was dissolved in PBS and 4mg alum (Imject, Sigma) in a volume of 25 μL and injected into each hind footpad. For i.p. immunizations, 10μg of NP_{31}-KLH and dissolved in 4mg alum. NP_4- and NP_{25}-BSA (15 μg/mL Biosearch Technologies) were used to coat ELISA plates in PBS for high and low affinity NP-specific IgG_1. For blocking antibody experiments, mice were administered indicated amounts of a monoclonal ICOSL blocking antibody (MIL-5733)(17) i.p.

HDM model

HDM (Dermatophagoides and Teronyssinus) extracts were obtained from Greer Laboratories. Mice were administered intranasally (i.n) 25μg HDM extract dissolved in 25μL PBS daily for four days, with a ten day break, followed by an additional four intranasal immunizations. For restimulation of draining lymph nodes with HDM extract, medLN cells were isolated at day 20 and restimulated with indicated HDM concentrations at a

concentration of $2e^6$ cells/mL. Tag-It Violet (BioLegend) was used to measure proliferation by flow cytometry. For restimulation of T cells from lung tissue, lungs were digested using collagenase I, DNAse, and dispase I (Sigma) for 1 hour at 37°C. Digested tissue was passed through a 40 μm mesh and washed twice with PBS. T cells were restimulated with plate bound anti-CD3 (2μg/mL) for 4 hours in the presence of monensin. For T cell proliferation studies, T cells ($1e^6$/mL) were stimulated with 1μg/mL plate bound anti-CD3 for 72 hours.

Cell Culture

Isolated mouse and human B cells were cultured in cRPMI 1640 containing 10% FBS, 2mM L-glutamine, 100 U/mL penicillin, 100 ug/mL streptomycin, 1 mM HEPES, 1 mM sodium pyruvate, 2mM 2-mercaptoethanol, and 1μg/mL αCD40 (5). The M12 and 8866 cell lines were cultured in cRPMI 1640 containing 10% FBS, 2mM L-glutamine, 100 U/mL penicillin, 100 ug/mL streptomycin, 1 mM HEPES, and 1 mM sodium pyruvate. GI254023X (Sigma) used at the concentration of 1μM is considered specific for ADAM10 and is above the published IC_{50} of 5nM (18, 19).

Cell Isolation

Spleens were homogenized and passed through a 40 μm mesh. Erythrocytes were lysed using ammonium-chloride-potassium lysing buffer (Quality Biologic). B cells were isolated using B220 positive selection (Miltenyi Biotec, Auburn, CA, USA), according to manufacturer's protocol. $CD4^+$ T cell isolation was conducted using negative selection (Biolegend), according to manufacturer's protocol. Human tonsillar B cells were isolated by creating a single cell suspension followed by IgD positive selection.

Immunohistochemistry

Ten micron frozen sections were cut from the excised mouse LNs, fixed in absolute acetone, air-dried, and blocked with serum-free protein block (X0909; Dako) as described. Sections were labelled with PE conjugated rat anti-mouse ICOSL (clone HK5.3, Biolegend, 107405), unconjugated rabbit anti-mouse ICOS (Abcam, ab138354) followed by PE conjugated-Fab2 donkey anti-rabbit IgG, Alexa Fluor 647 conjugated rat anti-mouse CD45R/B220 (clone RA3-6B2, Biolegend, 103226), Alexa fluor 488 conjugated rat anti-mouse CD4 (Clone GK1.5, Biolegend, 100423), anti-mouse Lyve-1 eFluor 660 (Clone ALY7, eBioscience, 50-0443-82) and FITC conjugated-GL7 (GL7, BD Pharmingen, 562080). The Ab concentrations ranged between 5 and 10 μg/mL. Sections were mounted with antifade mounting medium, Vectashield (Vector Laboratories), cover-slipped, and examined with a Leica TCS-SP2 AOBS confocal laser-scanning microscope. Three lasers were used 488, 543 and 633 nm; far red emission is shown as pseudo blue. Parameters were adjusted to scan at 1024 × 1024 pixel density and 8-bit pixel depth. Emissions were recorded in three separate channels, and digital images were captured and processed with Leica Confocal, LCS Lite software.

EAE induction

Active EAE was induced as previously described [19]. Briefly, 200μg MOG_{35-55} was dissolved in PBS and emulsified in CFA with 4mg/mL heat-inactivated *M. tuberculosis*

extract. Mice were immunized at four locations (50μL each) on the hind flanks. Pertussis toxin was administered *i.p.* on days 0 and 2. Mice were observed daily and clinical scores were as follows: 0: no clinical signs. 1: paralyzed tail. 2: hind limb paresis/loss of coordinated movement. 3: both hind limbs paralyzed. 4: forelimbs paralyzed. 5: moribund. For restimulation experiments, cells were isolated from the draining lymph node and cultured with increasing concentrations of MOG_{35-55}. Cells were incubated at 37C for 90 hours. Tag-It Violet (BioLegend) was used to measure proliferation by flow cytometry. For T cell intracellular cytokine staining following MOG restimulation, monensin was added in the last 6 hours of culture.

CRISPR/Cas9 Knockouts

RPMI 8866 were transfected with a modified pX330-U6-Chimeric_BB-CBh-hSpCas9 [Feng Zhang (Addgene plasmid # 42230)] plasmid (21) containing GFP. Cells were transfected using lipofectamine and single cell sorted 3 days later. Colonies were grown to confluency and screened for ADAM10 by flow cytometry. Short guide RNA (sgRNA) sequences are as follows: Adam10_sg1: 5′-AATTCTGCTCCTCTCCTGGG-3′; Adam10_sg2: 5′-TTTCAACCTACGAATGAAGA-3′.

Results

ADAM10 is the constitutive regulator of ICOSL levels

Our lab has previously shown that $ADAM10^{B-/-}$ mice have disrupted GC morphology and decreased T_{FH} development following immune activation (5). Given the importance of co-stimulatory signals in T cell activation, abnormal expression of CD80, CD86, CD40, ICOSL, and OX40L was investigated using our previously described $ADAM10^{B-/-}$ mice. Only ICOSL was found to be dysregulated. Expression was approximately 15-fold higher on $ADAM10^{-/-}$ B cells compared to WT (Fig. 1a; Supplemental Fig. 1a). Interestingly, while we found an increase in ICOSL surface expression, mRNA levels for *Icosl* dropped significantly (Fig. 1b). Given that ADAM17 has been reported to be involved in ICOSL shedding (16) we also examined B cells that lacked ADAM17 ($ADAM17^{B-/-}$) as well as B cells from $ADAM10/17^{B-/-}$ mice. Consistent with previous results, there was no difference in ICOSL levels on $ADAM17^{-/-}$ B cells compared to WT (Supplemental Fig. 1b). However, a modest but significant further increase in ICOSL was observed in $ADAM10/17^{-/-}$ B cells (Fig. 1a).

We next wanted to investigate ICOSL regulation in human B cells. The human lymphoblastoid cell line 8866 (22) was found to have high surface expression of ADAM10, but little ICOSL expression, (Fig. 1c) thus this cell line was a good candidate to test the effect of ADAM10 deletion. Using CRISPR-Cas9 8866 cells to delete ADAM10 (Supplemental Fig. 1c), ICOSL levels were enhanced above control 8866 when using two different guide RNAs to limit the chance of off-target effects (Fig. 1c). Next, human tonsillar B cells or WT mouse B cells were treated with an ADAM10-specific inhibitor (GI254023X) (18) and a time-dependent increase in surface ICOSL (Fig. 1d–f) was seen. CD40 stimulation is known to induce an increase in ICOSL expression (23) and thus, the data are normalized to the CD40 stimulation alone. This may explain why the increase in ICOSL

with inhibitor treatment was only 1.5-fold greater vs. 15-fold greater in ADAM10$^{B-/-}$ mice compared to WT mice (Fig. 1a,c *vs.* Fig. 1e,f)).

ADAM10 and ADAM17 directly cleave ICOSL but differentially regulate it at the cell surface

Given the above results and a previous report (16) that ADAM17 may be involved in the regulation of ICOSL, we sought to conclusively determine whether ADAM10 and ADAM17 can directly cleave ICOSL. To test this, recombinant mouse (rm) ICOSL was incubated with rmADAM10 or rmADAM17. After cleavage, N-linked glycosylation was removed with PNGase and blotting was performed with either anti-ICOSL (Fig. 2b) or anti-His tag (present on the carboxy terminus; Fig. 2a). Both blots indicated the release of a small, 3kDa fragment from the N-terminus (Fragment 1, Fig. 2a). Additionally, there were several sequential cleavage events, as there are multiple band shifts present, with the amino-terminal fragments estimated at 3.3 kDa, 6 kDa (Fragment 2, Fig. 2a) and 10 kDa (Fragment 3, Fig. 2b). rADAM17 was also His-tagged and explains the multiple bands present in lane 3 (Fig. 2a). These small fragments were not recognized by either antibody; they are either further degraded or do not have epitopes for the anti-ICOSL antibody. Additionally, an ADAM10 inhibitor (GI254023X) blocked the cleavage of ICOSL by ADAM10 (data not shown). Thus, both ADAM10 and ADAM17 can cleave ICOSL, when purified components are used. Blotting with anti-ICOSL (Fig. 2b) gave an additional 16kDa fragment being visible (Fig. 2b, fragment 3).

While ADAM10 and ADAM17 were both able to cleave recombinant ICOSL, we used various stimuli to tease apart the roles of each protease in the regulation of cell-bound ICOSL. Consistent with a previous report(16), treatment of purified WT B cells with PMA resulted in reduced ICOSL shedding in ADAM17$^{-/-}$ and ADAM10/17$^{-/-}$ B cells compared to WT (Fig. 2c), confirming a role for ADAM17 in the PMA-stimulated ICOSL shedding. The increase in shedding for ADAM10$^{B-/-}$ vs WT was expected since ADAM17 levels are increased on these cells (24). Ionomycin is known to activate ADAM10, while only slightly activating ADAM17 (1). Correspondingly, shedding of ICOSL on ionomycin-treated ADAM10$^{-/-}$ B cells was significantly less than WT B cells. Shedding on ADAM10/17$^{-/-}$ B cells was even further reduced (Fig. 2d). Next we stimulated purified B cells with α-hemolysin (HLA) which selectively binds to and activates ADAM10 (25, 26). Treatment with HLA triggered approximately 50% shedding of ICOSL in WT B cells, while shedding was essentially absent in ADAM10$^{-/-}$ B cells (Fig. 2e).

Of the stimulations known to cause ICOSL ectodomain shedding, engagement of ICOSL with ICOS is the most physiologically relevant, and indeed ICOS$^{-/-}$ mice have elevated ICOSL levels (27, 28). This interaction is known to cause rapid shedding of ICOSL from the cell surface (29). WT and ADAM17$^{-/-}$ B cells incubated for one hour with plate-bound ICOS caused approximately 27% of ICOSL to be shed from the cell surface (Fig. 2f). In contrast, ADAM10$^{-/-}$ B cells shed approximately 5% of ICOSL (Fig. 2f). Interestingly, ADAM10/17$^{-/-}$ B cells were completely protected from ICOSL shedding in response to ICOS engagement (Fig. 2f). Taken together, these results suggest that ADAM10 is the primary sheddase in response to ICOS engagement. However, ADAM17 appears to have a

more limited role in regulation of ICOSL in response to ICOS engagement in the absence of ADAM10.

ICOSL shedding is required for proper T cell ICOS regulation

Given the importance of the ICOS/ICOSL interaction for humoral immunity, it was counterintuitive that elevated ICOSL on ADAM10$^{-/-}$ B cells would result in the reduced T_{FH} differentiation and antibody response seen in these mice (5). We thus considered that inability to shed ICOSL may be altering ICOS expression. Indeed, splenic T cells from ADAM10$^{B-/-}$ mice have undetectable surface ICOS expression (Fig. 3a). Within the different T cell subsets, ICOS is most highly expressed on T_{FH} cells. When we examined the few T_{FH} present in draining LNs from either the ADAM10$^{B-/-}$ or ADAM10/17$^{B-/-}$ mice (Supplemental Fig. 2a–b), in contrast to total T cell analysis (Fig. 3a), ICOS surface levels were detectable but dramatically reduced compared to WT, while loss of ADAM17 alone had no effect on T_{FH} levels. Regulatory T_{FH} (T_{FR}) have been shown to alter T_{FH} responses (30), possibly explaining the decreased T_{FH} seen in ADAM10/17$^{B-/-}$ mice. However, we saw no differences in T_{FR} numbers following NP-KLH in alum immunizations (Supplemental Fig. 2c). When WT CD45.1^{+} T cells were adoptively transferred into CD45.2^{+} ADAM10$^{B-/-}$ recipient mice and ICOS surface expression levels monitored, donor CD45.1^{+} T cells lost ICOS surface expression within 24 hours and this loss of surface expression was maintained for up to 7 days (Figs. 3b, c). Since ICOS expression on developing T cells in the thymus was not altered (Supplemental Figs. 2d–e), we concluded that changes in expression occur in the periphery and requires continual interaction with elevated B cell ICOSL. Further evidence for regulation by ligand:receptor interaction is seen when T cell ICOS from ADAM10$^{B-/-}$ mice is restored to WT levels when stimulated *ex vivo* with anti-CD3 for three days (Fig. 3d). Next, we wanted to examine whether elevated ICOSL on B cells from ADAM10$^{B-/-}$ mice would directly down-regulate WT T cell ICOS levels *in vitro*. Co-culturing WT T cells with ADAM10$^{-/-}$ B cells led to a significant decrease in T cell ICOS levels within 24 hours (Fig. 3e). This decrease was blocked by addition of MIL-5733 (17, 31), a non-depleting ICOSL blocking antibody (Fig. 3e).

ICOS is internalized in response to ICOSL engagement

To determine the mechanism of this ICOS down-regulation, *Icos* transcription levels were examined and no differences were seen between WT and ADAM10$^{B-/-}$ T cells (Fig. 4a) suggesting that regulation occurs at the protein level. When surface and internal ICOS levels were examined by flow cytometry, T cells from ADAM10$^{B-/-}$ mice exhibited an elevated internal ICOS ratio relative to WT T cells (Fig. 4b, c) with essentially all the ICOS internalized. Using Amnis ImageStream analysis, we confirmed internalization of ICOS (Fig. 4d) by both WT and ADAM10$^{B-/-}$ T cells. The ICOS staining for WT T cells indicates some punctate internal spots, but most ICOS is surface expressed, while the ADAM10$^{B-/-}$ T cells have bright internal spots for ICOS staining. Examination of the internalization index with ImageStream software confirms an increased internalization in ADAM10$^{B-/-}$ compared to WT T cells (Fig. 4e). Together, these results indicate a novel regulation of ICOS through internalization following ligand interaction. This interaction occurs as the cells circulate through the secondary lymphoid system. In WT T cells, this interaction causes

ICOSL cleavage with some ICOS internalization, while in ADAM10$^{B-/-}$ mice, ICOS internalization is enhanced in T cells due to the inability of ADAM10 to cleave ICOSL.

Increased ICOSL on ADAM10$^{-/-}$ B cells is responsible for the attenuated antibody production

We wanted to directly demonstrate that altered ICOS/ICOSL interactions in ADAM10$^{B-/-}$ mice were responsible for the decreased humoral response by performing rescue studies. MIL-5733 is a blocking anti-ICOSL antibody (32) that can completely block ICOSL *in vivo* when administered at a dose of 150 μg every other day (17). We administered a sub-optimal dose (10 μg/mouse) of MIL-5733 every other day which we hypothesized would reduce the level of exposure of ICOSL to T cells in ADAM10$^{B-/-}$ mice (Fig. 5a). Within 48 hours of this dosing regimen, both unblocked ICOSL (Fig. 5b) and ICOS (Fig. 5c) were returned to levels seen in WT mice. To determine if the humoral response in ADAM10$^{B-/-}$ mice was restored, MIL-5733 was administered two days prior to footpad and intraperitoneal (*i.p.*) injections of NP_{31}-KLH and continued every other day. 14 days post-immunization GC B cells were significantly higher in ADAM10$^{B-/-}$ mice receiving the blocking antibody compared to isotype control (Fig. 5d, e). T_{FH} numbers were also significantly increased in ADAM10$^{B-/-}$ mice receiving the blocking antibody compared to isotype control (Fig. 5f, g) and within the recovered T_{FH} population, ICOS levels were similar to that seen in WT mice (Fig. 5h, i). Immunofluorescent microscopy analysis from of MIL-5733 treated ADAM10$^{B-/-}$ draining lymph nodes (dLN) indicates at least partial recovery of GCs by number and size (Supplemental Fig. 3a, b). Furthermore, antibody production was rescued, as total- (NP_{25}) and high-affinity (NP_4) IgG_1 levels were not significantly different between MIL-5733 treated ADAM10$^{B-/-}$ and WT mice while ADAM10$^{B-/-}$ receiving the isotype had significantly less total- and high-affinity IgG_1 (Fig. 5j).

Shedding of ICOSL is necessary for proper T cell responses

We have previously reported decreased T_H2 responses in ADAM10$^{B-/-}$ mice (6). With the above results, we hypothesized that this defect in T_H2 responses may be a result of elevated ICOSL in these mice. To investigate this, we decided to use ADAM10/17$^{B-/-}$ mice because they lack both physiological sheddases and therefore have the most elevated ICOSL levels. Using the house dust mite (HDM) model of Ballesteros-Tato et al. (33) (Supplemental Fig. 4a), we demonstrated reduced T_{FH} in the mediastinal lymph nodes (medLN) on day 6 (Supplemental Fig. 4b) as well as reduced T_H2 responses in lung T cells on day 20 (Figs. 6a–d). Thus, both T_{FH} and T_H2 are reduced in ADAM10/17$^{B-/-}$ mice as was seen in ADAM10$^{B-/-}$ mice. Furthermore, when day 20 medLN cells were cultured with increasing doses of HDM antigen, T cells from ADAM10/17$^{B-/-}$ mice had decreased proliferation (Fig. 6e), indicating less T cell activation. Together, these results suggest that inability to shed ICOSL is the primary mechanism behind the dysfunctional T_H2 responses in a HDM model.

In spite of the reduced responses seen in the HDM model, dLN cellular expansion was not different from WT mice (data not shown). To explore potential differential T cell activation, we utilized the active experimental autoimmune encephalomyelitis (EAE) model which is driven by both T_H1 and T_H17 activation (20, 34). ADAM10/17$^{B-/-}$ mice succumbed to more severe disease and higher incidence than WT mice (Fig. 7a, b). While central nervous

system (CNS) $CD4^+$ T cell levels and dLN cell numbers were not significantly different (Supplemental Fig. 4c, d), T_{FH} and GC B cell numbers were strongly reduced in ADAM10/17$^{B-/-}$ mice (Supplemental Figs. 4e–h), suggesting the possibility for enhanced T_H1 and/or T_H17 polarization of $CD4^+$ T cells. In support of this, clear increases in the levels of IFNγ^+ $CD4^+$ T cells were present in both the CNS (Fig. 7c, d) and the dLNs (Fig. 7e, f). While we did not see a difference in the number of IL-$17A^+$ T cells (Fig. 7g–j), re-stimulation of dLN cells with MOG_{35-55} led to enhanced IL-$17A^+$ (Fig. 7k) and IFNγ^+ (Fig. 7l) T cell levels in ADAM10/17$^{B-/-}$ mice compared to WT. Additionally, re-stimulation of dLNs with MOG_{35-55} caused a higher dose-dependent increase in proliferation by ADAM10/17$^{B-/-}$ T cells (Fig. 7m), in contrast to HDM restimulation. Overall the results demonstrate an affinity toward differentiation into T_H1 and T_H17 effector cells, while T_{FH} and T_H2 differentiation is attenuated.

Discussion

Defective humoral immune responses in ADAM10$^{B-/-}$ mice (5, 6) and an earlier report of ADAM17 being important for ICOSL shedding (16) prompted us to examine whether ADAM10 was involved in the shedding of ICOSL. Our studies demonstrate a large increase in ICOSL surface expression on B cells from ADAM10$^{B-/-}$ mice (Fig. 1a). While it had previously been reported that ADAM17 was involved in ICOSL release in response to PMA and BCR crosslinking (16), in agreement with Marczynska et al. (16) we did not see perturbation of ICOSL levels in ADAM17$^{B-/-}$ mice, supporting the presence of another protease. With interaction of ICOSL with ICOS most likely being the physiologic signal for cleaving ICOSL *in vivo*, we examined whether ADAM10 was the protease responsible for this regulation. ADAM10$^{-/-}$ B cells had reduced ICOSL shedding in response to ICOS ligation (Fig. 2f). Thus, in agreement with Marczynska et al (16), we conclude that ADAM17 cleaves ICOSL post-PMA or BCR interaction but ADAM10 is the protease responsible for ligand-induced as well as constitutive ICOSL shedding. This cleavage was further reduced in B cells from ADAM10/17$^{B-/-}$ mice, suggesting ADAM17 may have the capacity to act as a backup sheddase of ICOSL in the absence of ADAM10. In support of this, ADAM10/17$^{B-/-}$ mice further increased ICOSL levels *in vivo* compared to ADAM10$^{B-/-}$ mice (Fig. 1a). In addition, ICOSL cleavage was shown using recombinant proteins by examination of the fragment remaining after cleavage. Based on band shift analysis, recombinant protein assays suggest the primary fragment shed from the amino-terminus of ICOSL was approximately 3.3 kDa (Fig. 2a, b). Cleavage of this small fragment could result in disruption of tertiary structure preventing further ligation with ICOS. At least by size analysis, both ADAM10 and ADAM17 give similar sized fragments, although exact cleavage site analysis will be required to confirm this. Intriguingly, the cleavage of ICOSL has similarities to the S2 Notch1/2 cleavage. The interaction between Notch and its ligand exposes the cleavage site for ADAM10. ADAM17 is reported to cleave Notch, but the ADAM17 cleavage is primarily non-physiological. With the rapid kinetics of ICOSL shedding following interaction with ICOS, it would suggest that the increase in ICOSL shedding is due to activation of ADAM10 at a post-translational level. It will require further studies to determine whether interaction of ICOSL with ICOS causes signaling events to activate ADAM10 or whether ADAM10 is already associated near ICOSL and the

interaction of ICOS and ICOSL opens a cleavage site that is accessible to ADAM10, similar to Notch S2 cleavage (35). Perhaps a similar situation exists with ICOSL cleavage, namely, interaction with ICOS further exposes the ICOSL cleavage site. We note though, that HLA activation of ADAM10 results in efficient ICOSL cleavage indicating that highly activated ADAM10 does not need the ICOS interaction. We would argue that ADAM10 is responsible for both the low level, constitutive ICOSL cleavage seen in Figs. 1e,f as well as the ICOS induced cleavage (Fig. 2f).

The ICOS/ICOSL interaction has been shown to be particularly important in humoral immune function. Loss of this costimulatory axis largely blocks T_{FH} and T_H2 function (36). Understanding the regulation of both ICOS and ICOSL is essential for developing new approaches to modulate the antibody responses. While a number of ICOS regulatory mechanisms have been identified at the mRNA level (13, 15, 37), our studies demonstrate the importance of ICOSL shedding and ICOS internalization in control of this interaction. Indeed, T cell *Icos* transcriptional levels, were not different between ADAM10$^{B-/-}$ and WT T cells (Fig. 3a), confirming regulation of ICOS is at the protein level. As its name implies, ICOS is an induced costimulatory molecule but is still present at low levels on naïve T cells (11). When non-cleavable ICOSL is present, then ICOS levels become undetectable. Several studies have shown the flip side of this also occurs, namely, that alteration in ICOS levels can lead to dysregulation of ICOSL. In ICOS$^{-/-}$ mice, there is a marked increase in ICOSL levels on APCs (16, 28). Here we show that blocking the ICOSL catabolism gives rise to a phenotype similar to ICOS$^{-/-}$. While it may be possible that soluble ICOSL is causing the apparent downregulation of surface ICOS, we do not see a difference in thymic T cell ICOS levels, which would also be exposed to soluble ICOSL (Supplemental Fig. 2e). These results suggest that soluble ICOSL is not the mechanism behind decreased surface ICOS levels in ADAM10$^{B-/-}$ mice. Interaction between T cells and B cells in the secondary lymphoid tissue appears to be sufficient for this mechanism of ICOS:ICOSL regulation to occur.

One of the limiting factors of the GC response is the length of the initial ICOS/ICOSL interaction (38), which induces APC's to shed surface ICOSL (29, 38). Here we demonstrate that if ICOSL shedding is blocked, ICOS is internalized and degraded to a significant extent. It's important to note that ICOS internalization is also seen in WT T cells, though to a lesser extent, suggesting this is a normal control pathway for regulating surface ICOS/ICOSL expression. Loss of the capacity for this shedding, as seen in ADAM10$^{B-/-}$ and ADAM10/17$^{B-/-}$ mice, leads to a large accumulation of ICOSL on the B surface (Fig. 1a). To our knowledge, ICOSL is the only B7 family costimulatory molecule that is proteolytically cleaved upon receptor interaction. While internalization of CD28 may also play an important role in its regulation (39, 40), CD28 is also negatively regulated by CTLA4 which is able to bind the same ligands as CD28, which is unlike ICOS where ICOSL is only reported to interact with ICOS. The overall effect of this enhanced ICOSL expression is outlined in the model shown in Fig. 8.

The presence of such high ICOSL due to the loss of its primary sheddase resulted in loss of T_{FH} differentiation in several immunization models. In addition, we saw defective T_H2 responses in a HDM model of allergic asthma (6) (Figs. 6a–e). Thus, while we see the overall same reduction in T_H2 as *Ballesteros-Tato et al*, it is equally plausible that low ICOS

on the T resident memory cells (T_{RM}) would mean that both T_{FH} and T_{RM} models (41) could be operable here. The increased T_H1 and T_H17 responses seen in an active EAE model (Fig. 7) was reminiscent of the findings in $ICOS^{-/-}$ mice (9, 11). Indeed, expanded cellularity anticipated as a result of immunization was not significantly influenced with any of the immunization or disease models. Rather, increased $T_H1$and probably T_H17 activation now occurs. While blocking ICOSL resulted in recovery of ICOS, T_{FH} differentiation and GC formation, these studies were limiting in their ability to determine whether loss of GC formation was due to loss of ICOS costimulatory capacity or its ability to properly orient T cells to the germinal center (42).

Overall this study not only confirms the importance of ICOSL shedding in both ICOSL/ICOS function and expression, but it also identifies ADAM10 as the most important sheddase for controlling ICOSL levels. These results demonstrate how a normal regulatory pathway becomes aberrant when one of the required catabolism signals is not present. In addition, these findings demonstrate that blocking B cell ADAM10 activity represents a novel mechanism to modulate ICOSL and ICOS expression and alter the humoral immune response.

Supplementary Material

Refer to Web version on PubMed Central for supplementary material.

Acknowledgments

This study was funded by NIH/NIAID RO1AI18697A1-33-38 (to D.H.C.).

Flow cytometry was supported, in part, by Massey Cancer Center Core NIH Grant P30 CA16059. Matthew Zellner aided in mouse colony management. The modified PX330 plasmid containing GFP was a gift from Gordon Ginder and was developed by Xiaofei Yu. Alex Azzo aided in the development of $ADAM10^{-/-}$ RPMI 8226 and RPMI 8866 cell lines. We would also like to thank Jared Farrar for use of equipment.

References

1. Gall SML, Bobé P, Reiss K, Horiuchi K, Niu XD, Lundell D, Gibb DR, Conrad D, Saftig P, Blobel CP. ADAMs 10 and 17 Represent Differentially Regulated Components of a General Shedding Machinery for Membrane Proteins Such as Transforming Growth Factor α, L-Selectin, and Tumor Necrosis Factor α. Mol Biol Cell. 2009; 20:1785–1794. [PubMed: 19158376]
2. Möller-Hackbarth K, Dewitz C, Schweigert O, Trad A, Garbers C, Rose-John S, Scheller J. A Disintegrin and Metalloprotease (ADAM) 10 and ADAM17 Are Major Sheddases of T Cell Immunoglobulin and Mucin Domain 3 (Tim-3). J Biol Chem. 2013; 288:34529–34544. [PubMed: 24121505]
3. Gibb DR, Shikh ME, Kang DJ, Rowe WJ, Sayed RE, Cichy J, Yagita H, Tew JG, Dempsey PJ, Crawford HC, Conrad DH. ADAM10 is essential for Notch2-dependent marginal zone B cell development and CD23 cleavage in vivo. J Exp Med. 2010; 207:623–635. [PubMed: 20156974]
4. Weskamp G, Ford JW, Sturgill J, Martin S, Docherty AJP, Swendeman S, Broadway N, Hartmann D, Saftig P, Umland S, Sehara-Fujisawa A, Black RA, Ludwig A, Becherer JD, Conrad DH, Blobel CP. ADAM10 is a principal “sheddase” of the low-affinity immunoglobulin E receptor CD23. Nat Immunol. 2006; 7:1293–1298. [PubMed: 17072319]
5. Chaimowitz NS, Martin RK, Cichy J, Gibb DR, Patil P, Kang DJ, Farnsworth J, Butcher EC, McCright B, Conrad DH. A Disintegrin and Metalloproteinase 10 Regulates Antibody Production and Maintenance of Lymphoid Architecture. J Immunol. 2011; 187:5114–5122. [PubMed: 21998451]

6. Cooley LF, Martin RK, Zellner HB, Irani A-M, Uram-Tuculescu C, El Shikh ME, Conrad DH. Increased B Cell ADAM10 in Allergic Patients and Th2 Prone Mice. PLoS ONE. 2015; 10:e0124331. [PubMed: 25933166]
7. Mathews JA, Ford J, Norton S, Kang D, Dellinger A, Gibb DR, Ford AQ, Massay H, Kepley CL, Scherle P, Keegan AD, Conrad DH. A potential new target for asthma therapy: A Disintegrin and Metalloprotease 10 (ADAM10) involvement in murine experimental asthma. Allergy. 2011; 66:1193–1200. [PubMed: 21557750]
8. Choi YS, Kageyama R, Eto D, Escobar TC, Johnston RJ, Monticelli L, Lao C, Crotty S. ICOS Receptor Instructs T Follicular Helper Cell versus Effector Cell Differentiation via Induction of the Transcriptional Repressor Bcl6. Immunity. 2011; 34:932–946. [PubMed: 21636296]
9. Dong C, Juedes AE, Temann UA, Shresta S, Allison JP, Ruddle NH, Flavell RA. ICOS co-stimulatory receptor is essential for T-cell activation and function. Nature. 2001; 409:97–101. [PubMed: 11343121]
10. Hutloff A, Dittrich AM, Beier KC, Eljaschewitsch B, Kraft R, Anagnostopoulos I, Kroczek RA. ICOS is an inducible T-cell co-stimulator structurally and functionally related to CD28. Nature. 1999; 402:21–24.
11. Tafuri A, Shahinian A, Bladt F, Yoshinaga SK, Jordana M, Wakeham A, Boucher LM, Bouchard D, Chan VSF, Duncan G, Odermatt B, Ho A, Itie A, Horan T, Whoriskey JS, Pawson T, Penninger JM, Ohashi PS, Mak TW. ICOS is essential for effective T-helper-cell responses. Nature. 2001; 409:105–109. [PubMed: 11343123]
12. Akiba H, Takeda K, Kojima Y, Usui Y, Harada N, Yamazaki T, Ma J, Tezuka K, Yagita H, Okumura K. The Role of ICOS in the CXCR5+ Follicular B Helper T Cell Maintenance In Vivo. J Immunol. 2005; 175:2340–2348. [PubMed: 16081804]
13. Pratama A, Srivastava M, Williams NJ, Papa I, Lee SK, Dinh XT, Hutloff A, Jordan MA, Zhao JL, Casellas R, Athanasopoulos V, Vinuesa CG. MicroRNA-146a regulates ICOS-ICOSL signalling to limit accumulation of T follicular helper cells and germinal centres. Nat Commun. 2015; 6:6436. [PubMed: 25743066]
14. Jeltsch KM, Hu D, Brenner S, Zöller J, Heinz GA, Nagel D, Vogel KU, Rehage N, Warth SC, Edelmann SL, Gloury R, Martin N, Lohs C, Lech M, Stehklein JE, Geerlof A, Kremmer E, Weber A, Anders HJ, Schmitz I, Schmidt-Supprian M, Fu M, Holtmann H, Krappmann D, Ruland J, Kallies A, Heikenwalder M, Heissmeyer V. Cleavage of roquin and regnase-1 by the paracaspase MALT1 releases their cooperatively repressed targets to promote TH17 differentiation. Nat Immunol. 2014; 15:1079–1089. [PubMed: 25282160]
15. Di Yu A, Tan H-M, Hu X, Athanasopoulos V, Simpson N, Silva DG, Hutloff A, Giles KM, Leedman PJ, Lam KP, Goodnow CC, Vinuesa CG. Roquin represses autoimmunity by limiting inducible T-cell co-stimulator messenger RNA. Nature. 2007; 450:299–303. [PubMed: 18172933]
16. Marczynska J, Ozga A, Wlodarczyk A, Majchrzak-Gorecka M, Kulig P, Banas M, Michalczyk-Wetula D, Majewski P, Hutloff A, Schwarz J, Chalaris A, Scheller J, Rose-John S, Cichy J. The Role of Metalloproteinase ADAM17 in Regulating ICOS Ligand–Mediated Humoral Immune Responses. J Immunol. 2014; 193:2753–2763. [PubMed: 25108021]
17. Frey O, Meisel J, Hutloff A, Bonhagen K, Bruns L, Kroczek RA, Morawietz L, Kamradt T. Inducible costimulator (ICOS) blockade inhibits accumulation of polyfunctional T helper 1/T helper 17 cells and mitigates autoimmune arthritis. Ann Rheum Dis. 2010 annrheumdis119164.
18. Hundhausen C, Misztela D, Berkhout TA, Broadway N, Saftig P, Reiss K, Hartmann D, Fahrenholz F, Postina R, Matthews V, Kallen KJ, Rose-John S, Ludwig A. The disintegrin-like metalloproteinase ADAM10 is involved in constitutive cleavage of CX3CL1 (fractalkine) and regulates CX3CL1-mediated cell-cell adhesion. Blood. 2003; 102:1186–1195. [PubMed: 12714508]
19. Scholz F, Schulte A, Adamski F, Hundhausen C, Mittag J, Schwarz A, Kruse ML, Proksch E, Ludwig A. Constitutive Expression and Regulated Release of the Transmembrane Chemokine CXCL16 in Human and Murine Skin. J Invest Dermatol. 2007; 127:1444–1455. [PubMed: 17363916]
20. Stromnes IM, Goverman JM. Active induction of experimental allergic encephalomyelitis. Nat Protoc. 2006; 1:1810–1819. [PubMed: 17487163]

21. Chen S, Sanjana NE, Zheng K, Shalem O, Lee K, Shi X, Scott DA, Song J, Pan JQ, Weissleder R, Lee H, Zhang F, Sharp PA. Genome-wide CRISPR Screen in a Mouse Model of Tumor Growth and Metastasis. Cell. 2015; 160:1246–1260. [PubMed: 25748654]
22. Finegold I, Fahey JL, Granger H. Synthesis of Immunoglobulins by Human Cell Lines in Tissue Culture. J Immunol. 1967; 99:839–848. [PubMed: 4169031]
23. Liang L, Porter EM, Sha WC. Constitutive Expression of the B7h Ligand for Inducible Costimulator on Naive B Cells Is Extinguished after Activation by Distinct B Cell Receptor and Interleukin 4 Receptor–mediated Pathways and Can Be Rescued by CD40 Signaling. J Exp Med. 2002; 196:97–108. [PubMed: 12093874]
24. Folgosa L, Zellner HB, Shikh MEE, Conrad DH. Disturbed Follicular Architecture in B Cell A Disintegrin and Metalloproteinase (ADAM)10 Knockouts Is Mediated by Compensatory Increases in ADAM17 and TNF-α Shedding. J Immunol. 2013; 191:5951–5958. [PubMed: 24227779]
25. Powers ME, Kim HK, Wang Y, Wardenburg JB. ADAM10 Mediates Vascular Injury Induced by Staphylococcus aureus α-Hemolysin. J Infect Dis. 2012; 206:352–356. [PubMed: 22474035]
26. Wilke GA, Wardenburg JB. Role of a disintegrin and metalloprotease 10 in Staphylococcus aureus α-hemolysin–mediated cellular injury. Proc Natl Acad Sci. 2010; 107:13473–13478. [PubMed: 20624979]
27. Watanabe M, Takagi Y, Kotani M, Hara Y, Inamine A, Hayashi K, Ogawa S, Takeda K, Tanabe K, Abe R. Down-Regulation of ICOS Ligand by Interaction with ICOS Functions as a Regulatory Mechanism for Immune Responses. J Immunol. 2008; 180:5222–5234. [PubMed: 18390703]
28. Maazi H, Patel N, Sankaranarayanan I, Suzuki Y, Rigas D, Soroosh P, Freeman GJ, Sharpe AH, Akbari O. ICOS:ICOS-Ligand Interaction Is Required for Type 2 Innate Lymphoid Cell Function, Homeostasis, and Induction of Airway Hyperreactivity. Immunity. 2015; 42:538–551. [PubMed: 25769613]
29. Logue EC, Bakkour S, Murphy MM, Nolla H, Sha WC. ICOS-Induced B7h Shedding on B Cells Is Inhibited by TLR7/8 and TLR9. J Immunol. 2006; 177:2356–2364. [PubMed: 16887997]
30. León B, Bradley JE, Lund FE, Randall TD, Ballesteros-Tato A. FoxP3^{+} regulatory T cells promote influenza-specific Tfh responses by controlling IL-2 availability. Nat Commun. 2014; 5:ncomms4495.
31. Lischke T, Hegemann A, Gurka S, Van DV, Burmeister Y, Lam KP, Kershaw O, Mollenkopf HJ, Mages HW, Hutloff A, Kroczek RA. Comprehensive Analysis of CD4+ T Cells in the Decision between Tolerance and Immunity In Vivo Reveals a Pivotal Role for ICOS. J Immunol. 2012; 189:234–244. [PubMed: 22661090]
32. Weber JP, Fuhrmann F, Feist RK, Lahmann A, Baz MSA, Gentz LJ, Van DV, Mages HW, Haftmann C, Riedel R, Grün JR, Schuh W, Kroczek RA, Radbruch A, Mashreghi MF, Hutloff A. ICOS maintains the T follicular helper cell phenotype by down-regulating Krüppel-like factor 2. J Exp Med. 2015; 212:217–233. [PubMed: 25646266]
33. Ballesteros-Tato A, Randall TD, Lund FE, Spolski R, Leonard WJ, León B. T Follicular Helper Cell Plasticity Shapes Pathogenic T Helper 2 Cell-Mediated Immunity to Inhaled House Dust Mite. Immunity. 2016; 44:259–273. [PubMed: 26825674]
34. Miller, SD., Karpus, WJ., Davidson, TS. Experimental Autoimmune Encephalomyelitis in the Mouse. In: Coligan Al, John E., editor. Curr Protoc Immunol. Vol. CHAPTER. 2007.
35. Yuan JS, Kousis PC, Suliman S, Visan I, Guidos CJ. Functions of Notch Signaling in the Immune System: Consensus and Controversies. Annu Rev Immunol. 2010; 28:343–365. [PubMed: 20192807]
36. Crotty S. T Follicular Helper Cell Differentiation, Function, and Roles in Disease. Immunity. 2014; 41:529–542. [PubMed: 25367570]
37. Heissmeyer V, Vogel KU. Molecular control of Tfh-cell differentiation by Roquin family proteins. Immunol Rev. 2013; 253:273–289. [PubMed: 23550652]
38. Li J, Lu E, Yi T, Cyster JG. EBI2 augments Tfh cell fate by promoting interaction with IL-2-quenching dendritic cells. Nature. 2016; 533:110–114. [PubMed: 27147029]
39. Boomer JS, Green JM. An Enigmatic Tail of CD28 Signaling. Cold Spring Harb Perspect Biol. 2010:2.

40. Céfaï D, Schneider H, Matangkasombut O, Kang H, Brody J, Rudd CE. CD28 Receptor Endocytosis Is Targeted by Mutations That Disrupt Phosphatidylinositol 3-Kinase Binding and Costimulation. J Immunol. 1998; 160:2223–2230. [PubMed: 9498761]

41. Hondowicz BD, An D, Schenkel JM, Kim KS, Steach HR, Krishnamurty AT, Keitany GJ, Garza EN, Fraser KA, Moon JJ, Altemeier WA, Masopust D, Pepper M. Interleukin-2-Dependent Allergen-Specific Tissue-Resident Memory Cells Drive Asthma. Immunity. 2016; 44:155–166. [PubMed: 26750312]

42. Xu H, Li X, Liu D, Li J, Zhang X, Chen X, Hou S, Peng L, Xu C, Liu W, Zhang L, Qi H. Follicular T-helper cell recruitment governed by bystander B cells and ICOS-driven motility. Nature. 2013; 496:523–527. [PubMed: 23619696]

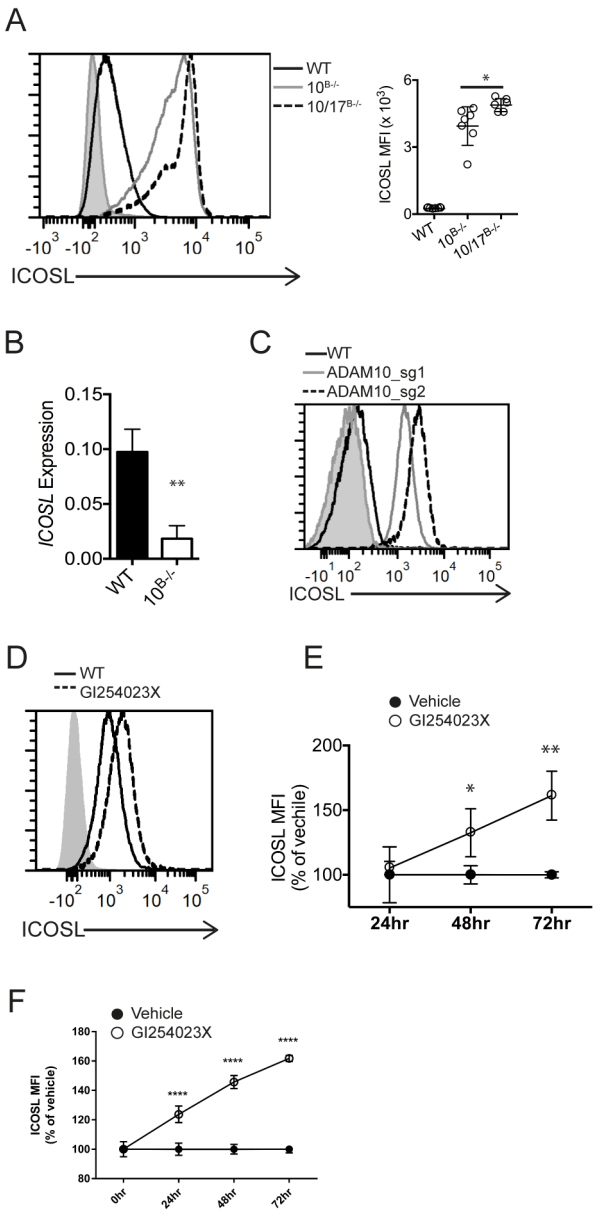

Fig. 1. ADAM10 regulates ICOSL on B cells

(A) Representative flow analysis of B cells from spleens of naïve WT, ADAM10$^{B-/-}$ and ADAM17$^{B-/-}$ mice and analysis of multiple samples shown at right of A. Isotype control staining is shaded gray. (B) qPCR analysis of *Icosl* expression from isolated splenic B cells, relative to *Hprt*. (C) Histogram of ICOSL levels on WT and ADAM10$^{-/-}$ RPMI 8866 cells. Isotype shading in grey. (D) Representative flow histogram of tonsillar IgD^{+} B cells stimulated with anti-CD40 for 72 hours in the presence of vehicle control or GI543023X. Isotype control staining is shaded gray. (E) Time course analysis of D. ICOSL MFIs were plotted vs. time relative to WT + vehicle control for each timepoint. (F) Splenic WT B cells were stimulated with anti-CD40 for indicated timepoints in the presence of vehicle or 1μM GI254023X, plotted as in E. **P < 0.05, **P < 0.01, ***P < 0.001* One-way ANOVA with

Tukey's post-test (A), Mann-Whitney U test (B), repeated measures ANOVA with Tukey's post-test (E – F). Data are pooled from three (A–F, mean ± s.d.) independent experiments.

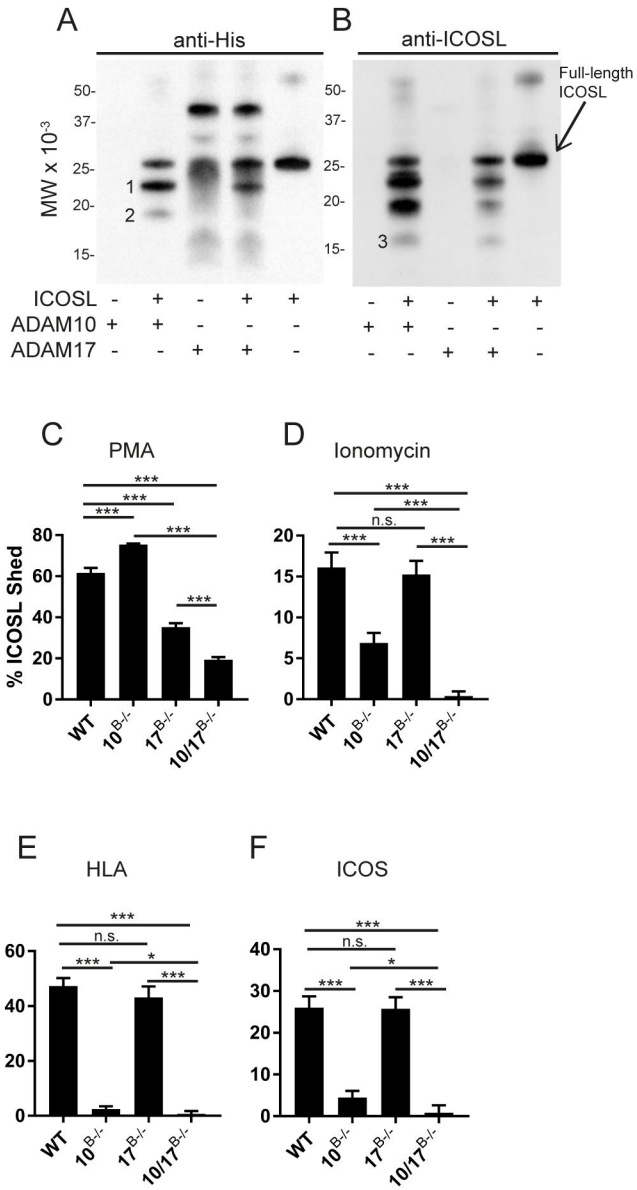

Fig. 2. ADAM10 and ADAM17 directly cleave ICOSL

(A–B) Western blot analysis of rmADAM10 or rmADAM17 incubated with rmICOSL, along with enzyme only controls, followed by PNGase deglycosylation and blotted for anti-His Tag (A) and anti-ICOSL (B). Position of intact deglycosylated ICOSL is shown and fragments generated by cleavage are numbered. (C–F) B cells were stimulated with PMA (C), α-hemolysin (HLA; D), ionomycin (E), or plate-bound ICOS (F) for 1 hour and %ICOSL shed from the cell surface was determined by flow cytometry relative to vehicle control stimulation (see materials and methods). *n.s., not significant ($P \geq 0.05$). *$P < 0.05$, ***$P < 0.001$, ****$P < 0.0001$* Kruskal-Wallis (A–D).

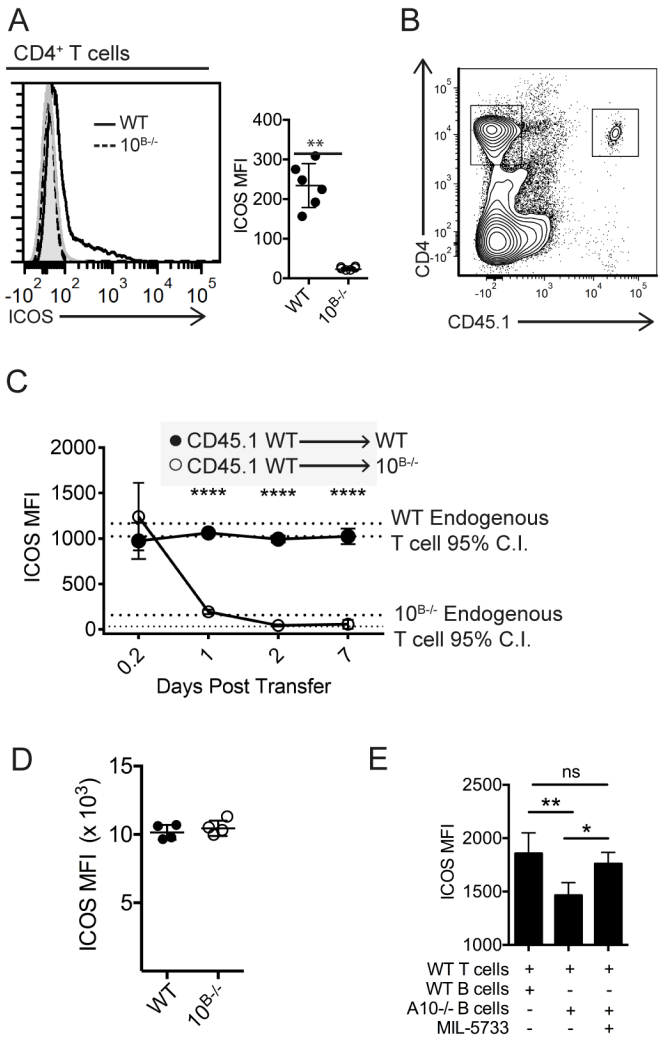

Fig. 3. ICOSL levels regulate ICOS levels *in vivo*

(A) Flow cytometry analysis of surface ICOS levels from splenic $CD4^+$ T cells in WT (black line) and $ADAM10^{B-/-}$ (red line) mice. Isotype control staining is shaded gray. (B,C) $5e^6$ $CD45.1^+$ WT T cells were adoptively transferred into $CD45.2^+$ WT or $CD45.2^+$ $ADAM10^{B-/-}$ mice and non-T_{FH} $CD4^+$ T cell ICOS levels were analyzed at indicated timepoints. Red dashed lines indicate the 95% C.I. of endogenous T cell ICOS levels in $ADAM10^{B-/-}$ mice and black dashed lines indicate the 95% C.I. of endogenous T cell ICOS levels in WT mice. (D) WT and $ADAM10^{B-/-}$ $CD4^+$ T cells were isolated and stimulated *in vitro* with 1μg anti-CD3 for three days and ICOS surface levels were determined by flow cytometry. (E) B cells from $ADAM10^{B-/-}$ or WT mice were isolated and cultured with WT $CD4^+$ T cells in the presence of an ICOSL blocking antibody (MIL-5733) or isotype control. ICOS levels on T cells were measured 24 hours later by flow cytometry. *n.s., not significant ($P \geq 0.05$), **$P < 0.01$, ****$P < 0.0001$* Unpaired Student's t-test (A, D), repeated measures analysis of variance (ANOVA) with Tukey's post-test (C), and one-way ANOVA (E). Data are pooled from two (A–E), mean ± s.d) independent experiments.

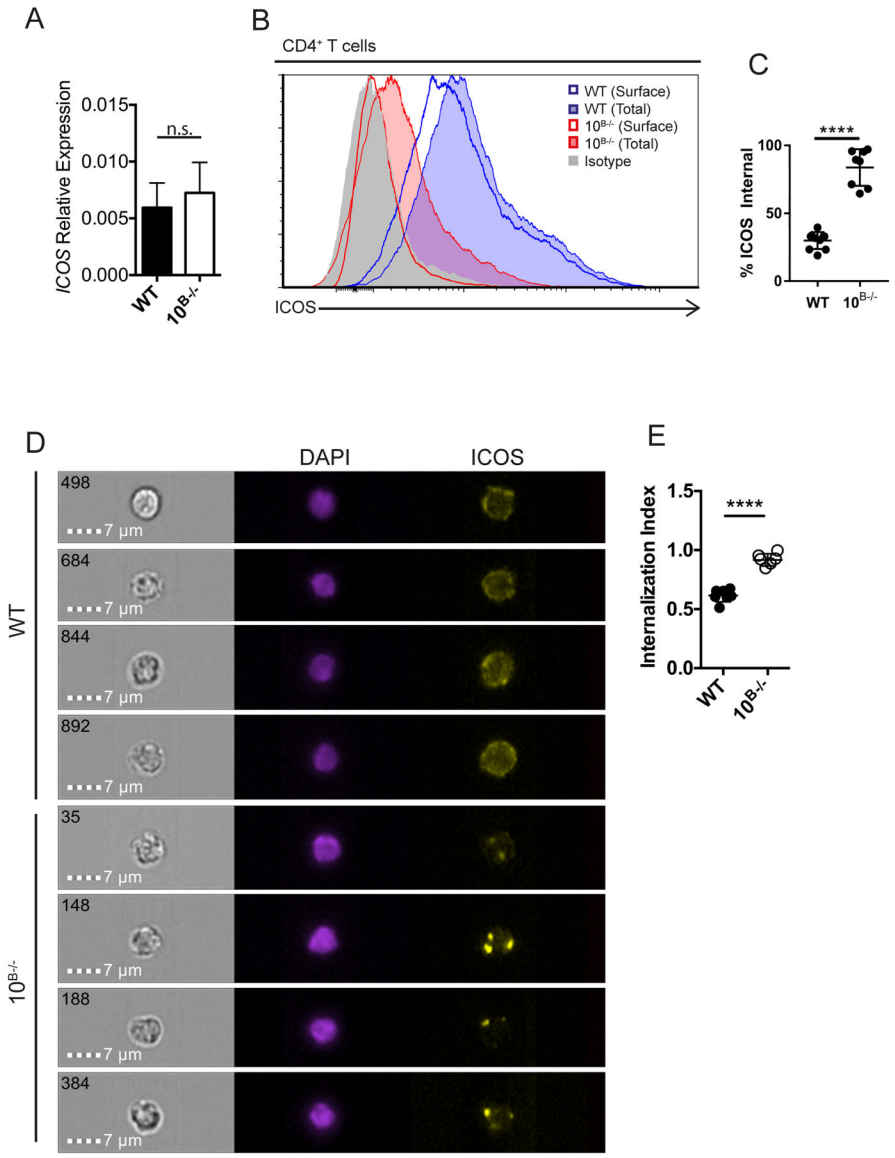

Fig. 4. T cells internalize ICOS in response to elevated ICOSL in ADAM10$^{B-/-}$ mice

(A) *Icos* mRNA levels were determined by qPCR on isolated CD4^{+} T cells from WT and ADAM10$^{B-/-}$ mice. (B, C) CD4^{+} T cells from WT and ADAM10$^{B-/-}$ mice were analyzed for surface (WT – blue line, ADAM10$^{B-/-}$ - red line) and total (surface $^{+}$ internal; WT – shaded blue, ADAM10$^{B-/-}$ - shaded red) ICOS levels by flow cytometry. Isotype control staining shaded gray. (C) % internal ICOS is represented as a % $ICOS_{Internal}$ = ($ICOS_{Total}$-$ICOS_{Surface}$)/$ICOS_{Total}$. (D) Representative images of splenic CD4^{+} T cells analyzed by ImageStream. (E) Internalization index was determined by internalization of ICOS into the nuclear plane (DAPI) as calculated by Amnis IDEAS software. *n.s., not significant ($P \geq 0.05$), *$P < 0.05$, ****$P < 0.0001$* Mann-Whitney U test (A) and unpaired Student's t-test (C, E). Data are pooled from two (A – E, mean ± s.d.) independent experiments.

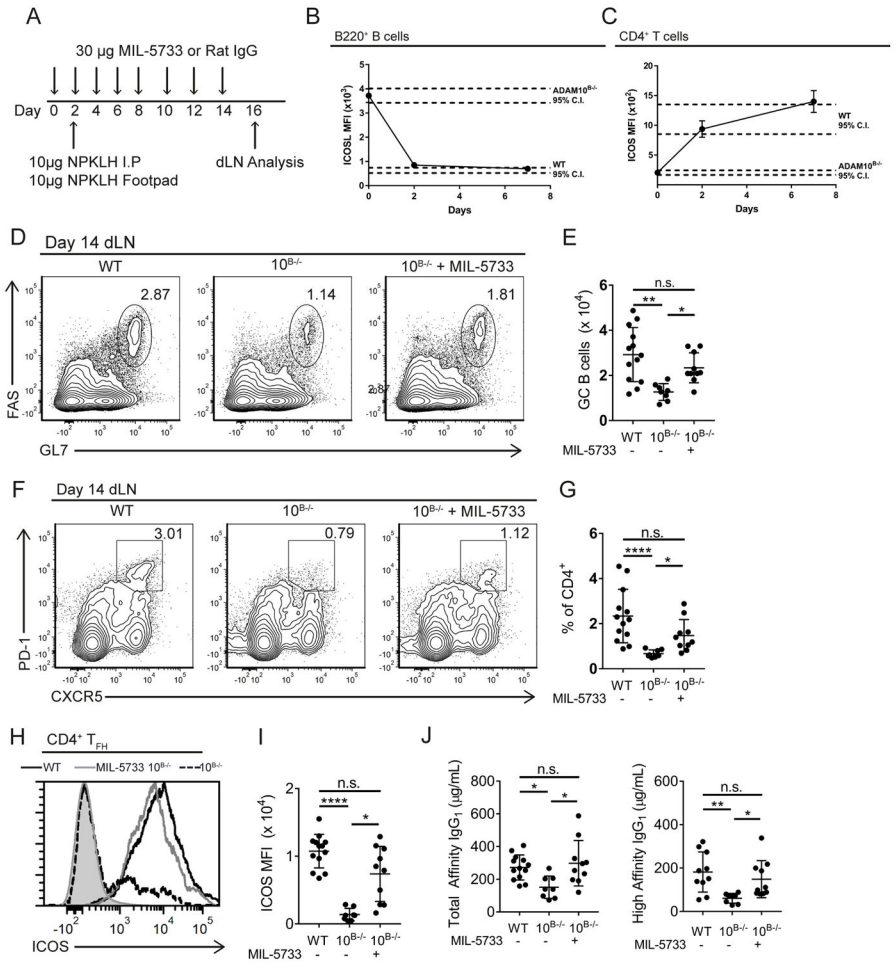

Fig. 5. Neutralization of high ICOSL levels in ADAM10$^{B-/-}$ restores germinal center B cells and antibody production

(A) model depicting antibody administration schedule and immunization strategy. (B–C) ADAM10$^{B-/-}$ mice were administered 30μg MIL-5733 every other day and ICOSL levels (B) on B cells and ICOS surface levels (C) on CD4^{+} T cells were measured by flow cytometry at indicated time points from the peripheral blood. (D–J) WT and ADAM10$^{B-/-}$ mice were administered MIL-5733 every other day and immunized with 10μg NP_{31}-KLH *i.p.* and in each hind footpad. Draining lymph nodes were analyzed for germinal center B cells (D – E) by flow cytometry as determined by CD95^{+} GL7^{hi} B cells and T_{FH} (F, G). (H) ICOS levels on T_{FH} from WT (black line), ADAM10$^{B-/-}$ (red line), and ADAM10$^{B-/-}$ + MIL-5733 (purple line) were determined by flow cytometry. Isotype control staining shaded gray. (I) quantification of H. (J) total and high affinity IgG_1 were determined by ELISA as in Materials and Methods. *n.s., not significant ($P \geq 0.05$). *$P < 0.05$, **$P < 0.01$, ***$P < 0.001$, ****$P < 0.0001$.* Kruskal-Wallis non-parametric test (A, E, G, I, J). Data are pooled from two (A – J mean ± s.d.) independent experiments.

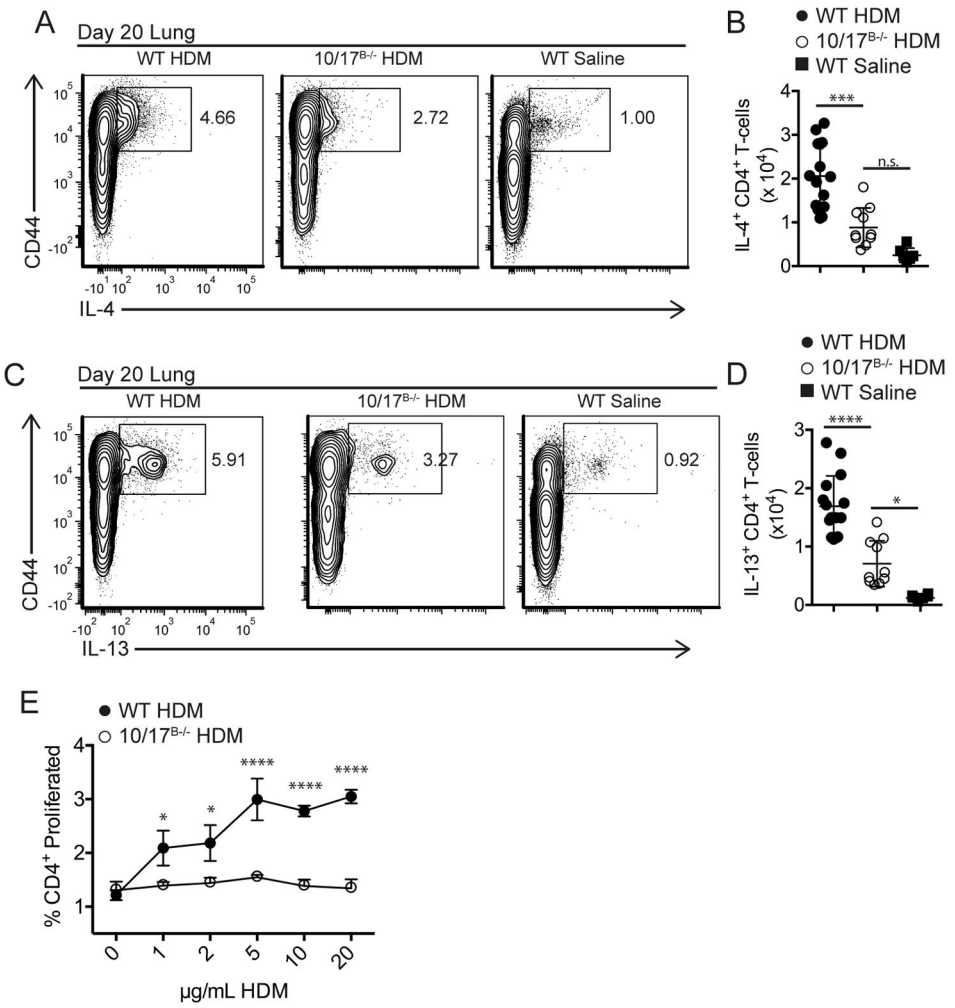

Fig. 6. ADAM10/17 $^{B-/-}$ mice have decreased T_H2 responses in a HDM allergic airway hypersensitivity model

(A–D) At day 20, lungs were digested as described in methods and stimulated with plate-bound anti-CD3 (2μg/mL) for 4 hours in the presence of monensin. Relative (A, C) and absolute (B, D) numbers of $IL4^+$ (A, B) and $IL13^+$ (C, D) effector T cells were determined by intracellular staining and flow cytometry. (E) medLN cells were isolated at day 20 and restimulated with increasing concentrations of HDM for 3 days. Proliferation was measured by cell trace violet. *n.s., not significant ($P \geq 0.05$). *$P < 0.05$, **$P < 0.01$, ***$P < 0.001$, ****$P < 0.0001$.* One-way analysis of variance (ANOVA) with Tukey's post-test (B, D), two-way ANOVA with Tukey's post-test (E). Data are pooled from three (A–E) independent experiments.

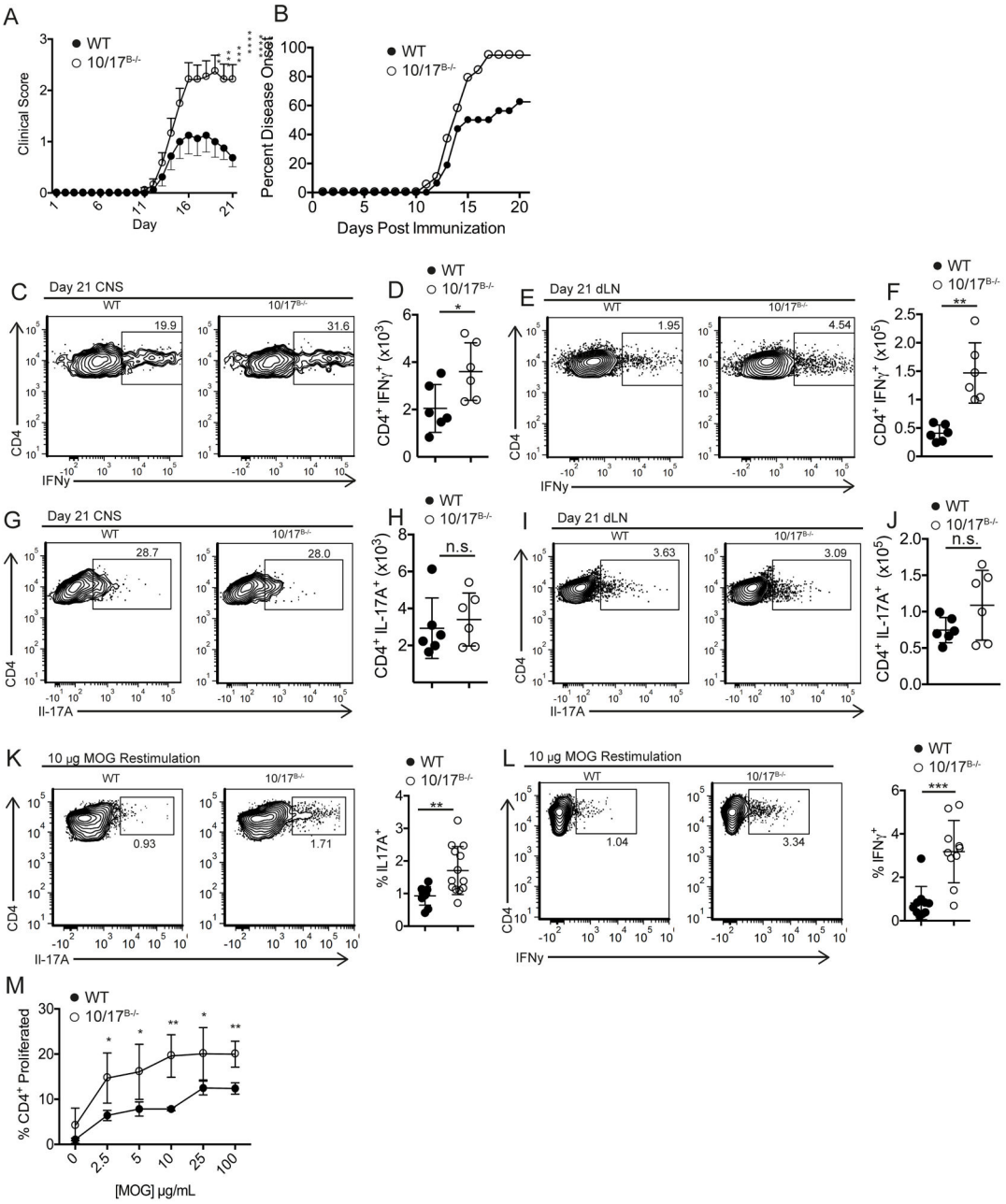

Fig. 7. ADAM10/17 $^{B-/-}$ mice have enhanced T_H1 and T_H17 responses

(A, B) WT and ADAM10/17$^{B-/-}$ mice had EAE induced using 200μg MOG_{35-55}. Clinical scores (A) and symptom incidence (B) were measured. (C, D, J, K) CNS tissue was analyzed at day 21 for $CD4^+$ $IFNg^+$ T cells (C, D) and $CD4^+$ IL-$17A^+$ T cells (J, K). (E, F, L, M) dLNs were analyzed at day 21 for $CD4^+$ $IFNg^+$ T cells (E, F) and $CD4^+$ IL-$17A^+$ T cells (L, M). (N, O) cells from day 21 dLN of EAE induced mice were restimulated with 10μg of MOG_{35-55} for 3 days and IL-17A (N) and IFNγ (O) expression was measured by flow cytometry. (P) Cells from day 21 dLN of EAE mice were isolated and restimulated with varying concentrations of MOG_{35-55} for 4 days in vitro and proliferation was measured

using cell trace violet. *n.s., not significant ($P \geq 0.05$). *$P < 0.05$, **$P < 0.01$, ***$P < 0.001$, ****$P < 0.0001$.* Two-way ANOVA with Tukey's post-test (P), repeated measures ANOVA (A, B), or unpaired Student's t-test (D, K, F, M, N, O). Data are pooled from three (A–P) independent experiments.

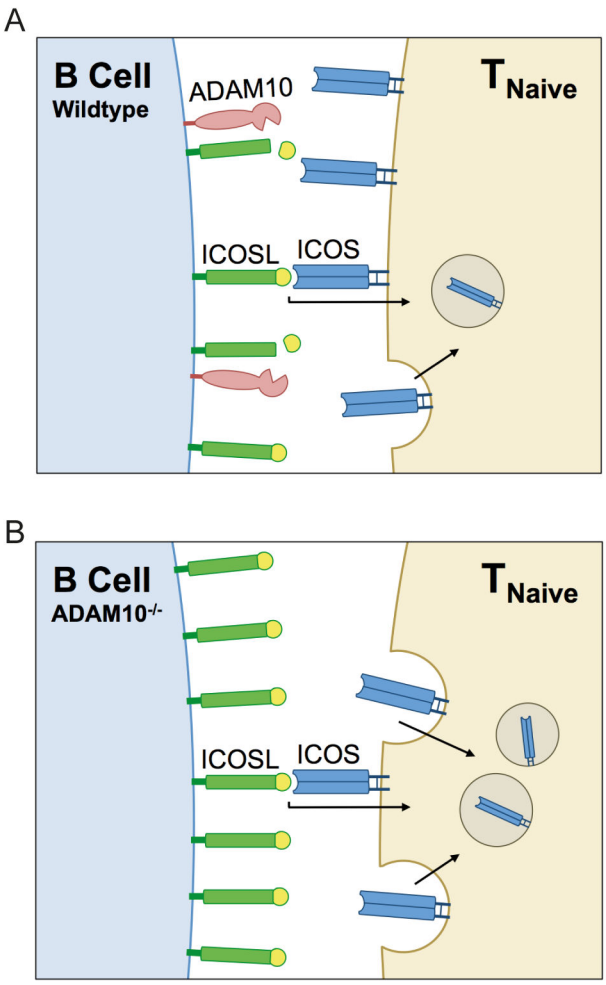

Fig. 8. Schematic of ADAM10-mediated ICOS/ICOSL regulation/mechanism

A) T cell ICOS interacts with B cell ICOSL in the secondary lymphoid organs. Upon ICOS/ICOSL interaction, ICOS is internalized to regulate the level on T cells. ADAM10 cleaves surface ICOSL to maintain low surface expression. B) When ADAM10 is knocked out on B cells, surface ICOSL accumulates because it is no longer being cleaved. Additionally, ADAM10$^{B-/-}$ B cells reduce the level of *Icosl* transcription. Higher levels of ICOSL leads to increased ICOS interaction, causing T cells to dramatically increase internalization of ICOS.